Inorganic Chemistry

ARTICLE

pubs.acs.org/IC

Dual Molecular Light Switches for pH and DNA Based on a Novel Ru(II) Complex. A Non-Intercalating Ru(II) Complex for DNA Molecular Light Switch

An-Guo Zhang, You-Zhuan Zhang, Zhi-Ming Duan, and Ke-Zhi Wang*

College of Chemistry, Beijing Normal University, Beijing 100875, P.R. China

Hui-Bo Wei, Zu-Qiang Bian, and Chun-Hui Huang

Beijing National Laboratory for Molecular Sciences, State Key Laboratory of Rare Earth Materials Chemistry and Applications, College of Chemistry and Molecular Engineering, Peking University, Beijing, 100871, China

Supporting Information

ABSTRACT: A new Ru(II) complex of $[Ru(phen)_2(Hcdpq)](ClO_4)_2$ {phen = 1,10-phenanthroline, Hcdpq = 2-carboxyldipyrido[3,2-*f*:2′,3′-*h*]quinoxaline} was synthesized and characterized. The spectrophotometric pH and calf thymus DNA (ct-DNA) titrations showed that the complex acted as a dual molecular light switch for pH and ct-DNA with emission enhancement factors of 17 and 26, respectively. It was shown to be capable of distinguishing ct-DNA from yeast RNA with this binding selectivity being superior to two well-known DNA molecular light switches of $[Ru(bpy)_2(dppz)]^{2+}$ {bpy =2,2′-bipyridine, and dppz = dipyrido-[3,2-*a*:2′,3′-*c*]phenazine}and ethidium bromide. The complex bond to ct-DNA probably in groove mode with a binding constant of $(4.67 \pm 0.06) \times 10^3\ M^{-1}$ in 5 mM Tris-HCl, 50 mM NaCl (pH = 7.10) buffer solution, as evidenced by UV−visible absorption and luminescence titrations, the dependence of DNA binding constants on NaCl concentrations, DNA competitive binding with ethidium bromide, and emission lifetime and viscosity measurements. To get insight into the light-switch mechanism, theoretical calculations were also performed by applying density functional theory (DFT) and time-dependent DFT.

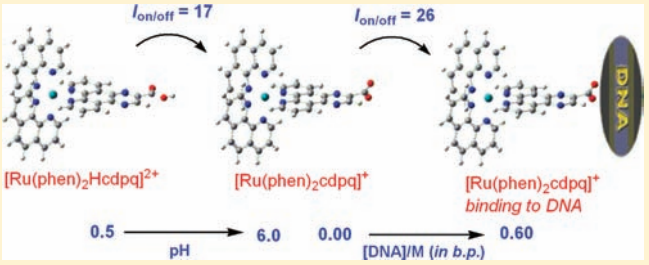

INTRODUCTION

Ru(II) polypyridyl complexes have been widely studied because of their intriguing photophysical, photochemical, and electrochemical properties as well as their widespread applications ranging from photosensitizers[1] to bioinorganic chemistry.[2−9] The DNA binding studies of these complexes have revealed structure−function relationships and many application prospects such as probes for DNA structure, DNA molecular light switches, DNA-dependent electron transfer probes, sequence-specific DNA cleaving agents, and anticancer drugs.[10] Barton and co-workers first reported that $[Ru(bpy)_2(dppz)]^{2+}$ and $[Ru(phen)_2(dppz)]^{2+}$ {bpy = 2,2′-bipyridine, phen = 1,10-phenanthroline, and dppz = dipyrido-[3,2-*a*:2′,3′-*c*]phenazine} acted as molecular light switches for DNA.[7,11,13,14] These complexes are almost nonemissive in DNA-free aqueous buffer, but became strongly emissive in the presence of double-stranded DNA. Since then, many derivatives of $[Ru(L)_2(dppz)]^{2+}$ (L = bpy or phen) have been synthesized by modifying the intercalative ligand dppz[4,8,12,14,15] to improve the DNA molecular light-switch properties. But usually these modified complexes showed poor light-switching properties compared to that of the parent complexes, as they usually exhibited residual emission in DNA-free water solution. In recent years, some researchers have turned their attention to the complexes containing dpq {dpq = dipyrido[2,2-*d*:2′,3′-*f*]-quinoxaline}, which is structurally related to but less conjugated than dppz. It was reported that $[Ru(phen)_2(dpq)]^{2+}$ and $[Ru(phen)_2(Me_ndpq)]^{2+}$ {*n* = 1, 2; Medpq = 2-methyldipyrido-[3,2-*f*:2′,3′-*h*]-quinoxaline; Me_2dpq = 2,3-methyldipyrido[3,2-*f*:2′,3′-*h*]-quinoxaline} exhibited strong luminescence in both the absence and the presence of DNA and did not show DNA light-switch behavior.[12,16−19] However, Ambroise and Maiya reported that $[Ru(phen)_2(dicnq)]^{2+}$ and $[Ru(phen)(dicnq)_2]^{2+}$ {dicnq = 6,7-dicyanodipyrido[2,2-*d*:2′,3′-*f*]quinoxaline} acted as DNA molecular light switches with emission intensity enhancement factors of 16 and 8, respectively.[18] Kelly and Kruger discovered that the incorporation of an amide group to dpq caused a major effect on the excited-state properties of its Ru(II) complex of $[Ru(phen)_2dpqa]^{2+}$ {dpqa = 2-pentylamidodipyrido-[3,2-*f*:2′,3′-*h*]-quinoxaline}, which did not emit in water but

Received: October 21, 2010
Published: June 22, 2011

Scheme 1. Synthetic Route to $[Ru(phen)_2(Hcdpq)]^{2+}$

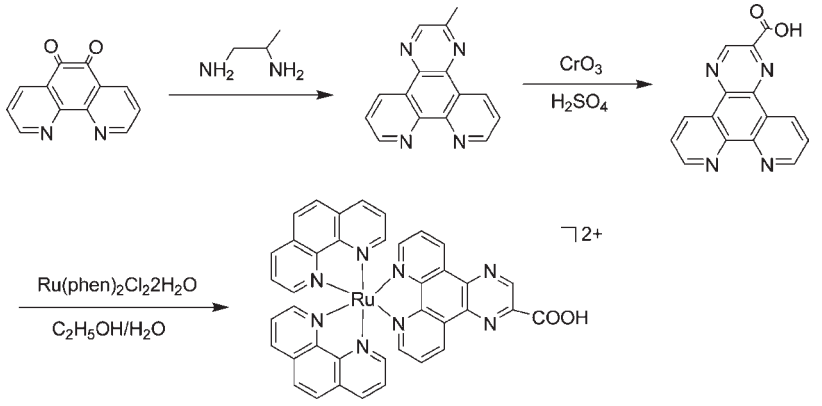

exhibited strong luminescence in DNA environment, thus acting as a good DNA molecular light-switch.[19] We have also reported three good DNA molecular light-switch complexes of $[Ru(bpy)_2(bipp)]^{2+}$, $[Ru(bpy)_2(bopp)]^{2+}$, and $[Ru(bpy)_2(btpp)]^{2+}$, which were synthesized by grafting of benzimidazoyl, benzoxazolyl, and benzthiazolyl moieties to $[Ru(bpy)_2(dpq)]^{2+}$, respectively.[20] Upon addition of calf thymus (ct-DNA), the emission intensities of these three complexes increased sharply by 49, 89, and 179 folds, respectively. The ancillary ligands were also found to play an important role in governing DNA light-switch behaviors.[21,22] It was reported that a phen-containing complex of $[Ru(phen)_2(taptp)]^{2+}$ {taptp = 4,5,9,18-tetraazaphenanthreno[9,10-*b*]triphenylene}[22] exhibited negligible luminescence in DNA-free water buffer, in contrast to the strong luminescence for a bpy-containing complex of $[Ru(bpy)_2(taptp)]^{2+}$.[21]

It is worthwhile to note that the DNA light-switch behaviors of transition metal complexes have almost always been identified as a characteristic of the DNA intercalators and regarded as confirmation of DNA intercalation.[9,12,23] However, a DNA molecular light switching dinuclear Ru(II) complex of $[(bpy)_2Ru(tpphz)Ru(bpy)_2]^{4+}$ {tpphz = tetrapyrido-[3,2-*a*:2′,3′-*c*:3″,2″-*h*:2″,3‴-*j*]phenazine} has challenged this principle. In 2005 Rajput et al. first reported that $[(bpy)_2Ru(tpphz)Ru(bpy)_2]^{4+}$ turned on its luminescence in the presence of DNA by intercalating between the DNA base pairs in a threading fashion with a DNA binding constant K_b value on the 10^4 M^{-1} order of magnitude.[15] The conclusion regarding intercalative DNA binding mode was drawn mainly from a slight increase in DNA viscosities by a factor of only 0.03 at [DNA bp]/[Ru] = 0.2. Dunbar and Turro and their co-workers have recently made a different conclusion that $[(bpy)_2Ru(tpphz)Ru(bpy)_2]^{4+}$ should be an electrostatic surface DNA binder as evidenced by a DNA melting experiment, reverse salt titrations, and viscosity measurements.[24] Furthermore, they pointed out that the increases of the DNA viscosities in the Rajput's study might be caused by the contamination of the complex with relatively small amount of $[Ru(bpy)_2(tpphz)]^{2+}$. To date, $[(bpy)_2Ru(tpphz)Ru(bpy)_2]^{4+}$ has been a first example of a nonintercalating light-switch metal complex for double-stranded DNA, providing the evidence that "intercalation is not absolutely required for DNA light-switch behavior".[24] Many experimental and theoretical efforts have also been made on the DNA "light-switch" mechanism.[25−33] The following four possibilities were reported to be potential causes of the DNA light switching behaviors observed: (1) the protection of the intercalative moieties from interacting with water by intermolecular hydrogen bonding, or excited-state proton-transfer, (2) a hydrophobic environment provided by the DNA, (3) the decrease in radiative vibrational relaxation by a rigid local environment of the intercalating Ru(II) complex, and (4) the presence of two ^{3}MLCT states: a bright, luminescent state associated with the bipyridine (bpy) fragment; and a dark, nonluminescent state localized largely on the phenazine (phz) portion.[25] In aprotic solvents, the lowest ^{3}MLCT state is a bright state (BS), and thus luminescence was observed. But in protic environments, the hydrogen bonding with the phz nitrogens lowered the energy of the dark state (DS) to below that of the BS,[28−30] and shutting off the luminescence by a decay process from the DS via nonradiative vibrational relaxation back to the ground state.[31,32] Turro and co-workers studied a series of DNA light switching ruthenium(II) complexes by density functional theory (DFT) and time-dependent DFT (TDDFT) calculations, providing the supporting evidence for the presence of the BS and DS. They also pointed out that the key to the light-switch behavior is the energy gap between the BS and the DS.[33]

On the other hand, many life processes, such as enzymes, operate within a very narrow pH window, where their function or activity can be described as being "on/off switching" as a function of pH.[34] The pH responsive transition-metal complexes containing *N*-heterocyclic ligands are one family of fundamental molecular devices with adjustable ground- and excited-state properties[35,36] and biological activities[37] by changing the pH of molecular environment. Of these complexes, Ru(II) complexes have received long-standing attention as pH sensors because of their long excited-state lifetimes and high luminescence quantum yields.[38−44] It is well-known that the grafting of protonatable/deprotonatable groups such as hydroxyl, carboxyl, and amino groups to Ru(II) complexes may make these complexes sensitive to the changes in environmental pH, and sequentially provide a chance to develop pH sensing/switching molecular devices,[39−44] and to greatly modulate their biological functionalities.[38,45]

In continuation of our efforts on acid−base and DNA binding properties of Ru(II) complexes,[20,39,40,43,44,46] we have synthesized a Ru(II) complex of $[Ru(phen)_2(Hcdpq)]^{2+}$ with a carboxylic group being grafted to the pyrazine ring of dpq. This complex was found to act as a dual luminescence switch for both pH and ct-DNA. The DNA light switch behavior was evidenced to be induced probably by a groove DNA binding. The DNA and RNA comparative binding luminescence spectroscopy studies

dx.doi.org/10.1021/ic102126m |*Inorg. Chem.* 2011, 50, 6425–6436

showed that this complex could distinguish the DNA from yeast RNA with the binding selectivity obviously superior to well-known DNA light switches of $[Ru(bpy)_2(dppz)]^{2+}$ and ethidium bromide. In this paper, we would like to report these interesting findings.

EXPERIMENTAL SECTION

Materials. 2-Carboxyldipyrido[3,2-*f*:2′,3′-*h*]quinoxaline (Hcdpq) and $[Ru(phen)_2Cl_2]\cdot 2H_2O$ were synthesized according to literature procedures.[47,48] Solvents were purified and dried according to the standard methods.[49] The synthetic route to $[Ru(phen)_2(Hcdpq)]^{2+}$ is shown in Scheme 1, and the synthetic details are given below. The other materials were obtained from commercial sources and used without further purification.

Synthesis of $[Ru(phen)_2(Hcdpq)](ClO_4)_2\cdot H_2O$. A solution of $[Ru(phen)_2Cl_2]\cdot 2H_2O$ (112.7 mg, 0.20 mmol) and Hcdpq (59.7 mg, 0.21 mmol) in ethylene glycol (4 mL) was heated at 110 °C under N_2 for 7 h. The reaction mixture was cooled to room temperature and filtered. Then a saturated $NaClO_4$ aqueous solution was dropwise added into the filtrate. The red-orange precipitate formed was filtered and recrystallized from CH_3CN/1,4-dioxane. (***Caution!*** *Perchlorate salts are potentially explosive and therefore should be handled in small quantity with care.*) Yield: 112.7 mg (57%). ^{1}H NMR (500 MHz, Me_2SO-d_6): 7.76−7.81(m, 4H), 7.89(q, 2H, J = 4.7 Hz), 8.07(d, 2H, J = 5.0 Hz), 8.21(d, 3H, J = 4.1 Hz), 8.26(d, 1H, J = 4.9 Hz), 8.40(s, 4H), 8.79(d, 4H, J = 7.5 Hz), 9.50(t, 2H, J = 10.3 Hz), 9.68(s, 1H). Anal. Found: C, 49.64; H, 3.25; N, 11.68. Calc. for $C_{39}H_{26}Cl_2N_8O_{11}Ru$: C, 49.06; H, 2.75; N, 11.74. Anal. Calc. for FAB-MS: m/z 837.19 $\{[-ClO_4^-]^+\}$ Found: m/z 837.20 $\{[-ClO_4^-]^+$.

Physical Measurements. Elemental analyses (C, H, and N) were performed on a Vario EL elemental analyzer. NMR spectra were collected on a Bruker DRX-500 NMR spectrometer with Me_2SO-d_6 as solvent. UV−visible spectra were obtained on a GBC Cintra 10e UV−visible spectrometer. Emission spectra were obtained on a Shimadzu RF-5301PC spectrofluorimeter. UV−visible and emission spectrophotometric pH titrations of the complex were carried out in Britton-Robinson buffer (40 mM H_3BO_3, 40 mM H_3PO_4, 40 mM CH_3COOH) with 0.1 M NaCl to keep constant ionic strength. The luminescence quantum yields were calculated by comparison with $[Ru(bpy)_3]^{2+}$ (φ_{std} = 0.033)[50] in aerated aqueous solution at room temperature using eq 1, where φ and φ_{std} are the quantum yields, A and A_{std} are the absorbances at the excitation wavelength, and I and I_{std} are the integrated emission intensities for the unknown and standard samples, respectively.

$$\varphi = \varphi_{std}(A_{std}/A)(I/I_{std}) \quad (1)$$

The photoluminescence lifetimes were determined by time-correlated single photon counting method on an Edinburgh FLS 920 spectrometer with an nF900 ns flash lamp with pulse width of 1 ns as the excitation source.

All the experiments involving the interaction of the complex with ct-DNA and the yeast RNA (Sigma Co., Type VI from Torula yeast) were carried out in aerated buffer (5 mM Tris-HCl, 50 mM NaCl, pH = 7.10 ± 0.02). A solution of DNA gave a ratio of UV absorbance at 260 and 280 nm of about 1.9:1, indicating that the DNA was sufficiently free of protein. The DNA concentration per base pairs was determined spectrophotometrically by assuming ε_{260} = 13200 M^{-1} cm^{-1}. The concentration of the yeast RNA was determined by assuming ε_{260} = 7800 M^{-1} cm^{-1}. Viscosity experiments used an Ubbelohde viscometer, immersed in a thermostatted water-bath maintained at 31.66 ± 0.01 °C. The DNA samples, approximately 200 base pairs in average length, were prepared by sonication to minimize complexities arising from DNA flexibility.[51] Data were presented as $(\eta/\eta_0)^{1/3}$ versus the ratio of the concentration of the Ru(II) complex to that of the DNA, where η and η_0 are the viscosities of DNA solutions in the presence and the absence of complex, respectively. Viscosity values were calculated from the observed flowing time of DNA containing solutions (t) corrected for that of buffer alone (t_0), $\eta = t - t_0$.[52]

Scheme 2. Structural Schematic Diagram of $[Ru(phen)_2(dpq)]^{2+}$ 1, $[Ru(phen)_2(Hcdpq)]^{2+}$ 2, and $[Ru(phen)_2(cdpq)]^{+}$ 3

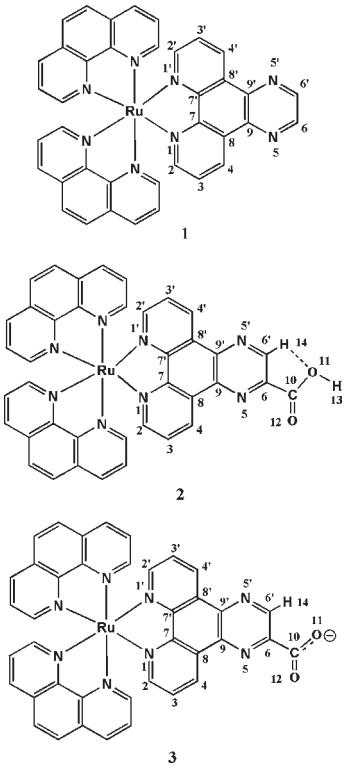

Computational Methods. $[Ru(phen)_2(Hcdpq)]^{2+}$ is made of one Ru(II), one main ligand (Hcdpq), and two ancillary ligands (phen), as shown in Scheme 1. There are 74 atoms involved in the complex which belongs to C_1 symmetry. Geometry optimization computations for the ground states of $[Ru(phen)_2(Hcdpq)]^{2+}$, deprotonated $[Ru(phen)_2(cdpq)]^{+}$, and the parent complex $[Ru(phen)_2(dpq)]^{2+}$ were performed in their singlet states.[53] The subsequent frequency analysis shows that the structures are local minima on the potential energy surface. Electronic structures and vertical singlet transition energies of $[Ru(phen)_2(Hcdpq)]^{2+}$ and $[Ru(phen)_2(cdpq)]^{+}$ were also obtained in water using DFT and time-dependent DFT (TDDFT), respectively, combined with the conductor-like polarizable continuum model (CPCM)[54,55] based on the geometry optimization results. All the computations were performed applying DFT (or TDDFT)-B3LYP method[56−58] with the 6-31G*[59] basis set for C, N, O, H atoms and LanL2DZ for the Ru atom[60,61] with the G03 quantum chemistry program-package.[62]

RESULTS AND DISCUSSION

Computational Studies. The molecular structures of $[Ru(phen)_2(dpq)]^{2+}$ **1**, $[Ru(phen)_2(Hcdpq)]^{2+}$ **2**, and $[Ru(phen)_2(cdpq)]^{+}$ **3** are shown in Scheme 2. Their selected calculated bond lengths and dihedral angles are compared in Table 1 together with previously reported experimental data for **1**.[17] We can see that the calculated coordination bond lengths (Ru−N) and angles for **1** are very close to the experimental values, indicating that the results of the full geometry optimization computations by the DFT method are reliable, although the

dx.doi.org/10.1021/ic102126m |*Inorg. Chem.* 2011, 50, 6425–6436

Table 1. Selected Calculated Bond Lengths (nm), Bond Angles (deg), and Dihedral Angels (deg) Using the DFT-B3LYP at the Lanl2dz/6-31G* Level

								dihedral angle	
complex		Ru−N_m[a]	Ru−N_{co}	C−C_m[b]	C−C_{co}	A_m[c]	A_{co}	N5−C6−C10−O11	N5−C6−C10−O12
$[Ru(phen)_2(dpq)]^{2+}$ **1**	calc	0.2124	0.2124	0.1399	0.1395	78.6	78.5		
	expt[17]	0.2053	0.2069			79.6	79.2		
$[Ru(phen)_2(Hcdpq)]^{2+}$ **2**		0.2124	0.2125	0.1399	0.1395	78.4	78.4	179.99	−0.01
$[Ru(phen)_2(cdpq)]^{+}$ **3**		0.2117	0.2122	0.1399	0.1352	79.1	78.6	122.40	−56.51

[a] Ru−N_m expresses the mean coordination bond length between Ru and N atoms of the main ligand L, and Ru−N_{co} expresses that between Ru and N atoms of the coligand (phen). [b] C−C_m expresses the mean bond length of the ring skeleton of the main ligand, and C−C_{co} expresses that of the coligand. [c] A_m expresses the mean coordination bond angle between central Ru and two N atoms of the main ligand, and A_{co} expresses that of the coligand

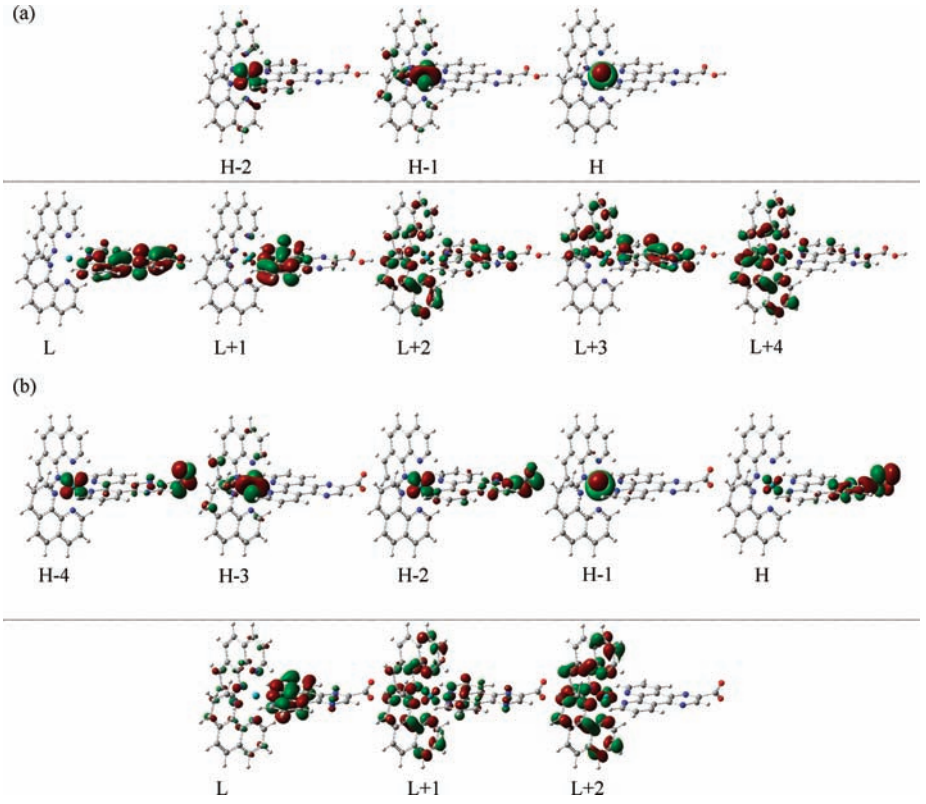

Figure 1. Contour plots of some frontier molecular orbitals of $[Ru(phen)_2(Hcdpq)]^{2+}$ **2** (a) and $[Ru(phen)_2(cdpq)]^{+}$ **3** (b) calculated by using the DFT-B3LYP method at LanL2DZ/6-31G* level.

computed and the experimental values for **2** could not be directly compared because the crystal structure of **2** has not yet been reported. The mean C−C bond lengths (0.1399 nm) for the main-ligands of dpq, Hcdpq, and cdpq on **1**−**3** are slightly longer than those (0.1392−0.1395 nm) of the coligand phen. The presence of carboxyl group on **2** does not make any substantial geometric changes with respect to **1.** The carboxyl group is well coplanar with dpq in **2** with the dihedral angles close to 0.00° or 180.00° (N5−C6−C10−O11 = −179.99°, and N5−C6−C10−O12 = 0.01°). The good planarity of Hcdpq in **2** can be attributed to the hydrogen bond formation between O11 and H14 (O11−H14 = 0.2440 nm). However, the deprotonation of **2** causes the rupture of hydrogen bond O11···H14−C6′ and the distortion of COO^- moiety, as illustrated by the dihedral angle values of 122.40° (N5−C6−C10−O11) and −56.51° (N5−C6−C10−O12) for **3** (see Scheme 2). This suggests that the main ligand cdpq in **3** has a relatively poor planarity, which might result in steric hindrance for cdpq to intercalate between DNA base pairs.

The components and energies of the frontier molecular orbital for **2** and **3** obtained by DFT calculations, are shown in Figure 1. For **2**, the highest occupied molecular orbital (HOMO), and the HOMO−1 and HOMO−2 are mainly characterized by the d orbitals of the Ru atom. The lowest unoccupied molecular orbital (LUMO) and LUMO+1 were found to be π^*_{Hcdpq} in character, and contributed by the whole Hcdpq ligand, and dominantly by the proximal bpy portion of Hcdpq, respectively (see Figure 1 a). Furthermore, the next three unoccupied molecular orbitals (LUMO+2, LUMO+3 and LUMO+4) were found to be an admixture of π^*_{Hcdpq} and π^*_{phen} in character. By contrast, the

dx.doi.org/10.1021/ic102126m |*Inorg. Chem.* 2011, 50, 6425–6436

Table 2. TDDFT Calculated Energies, Oscillator Strengths, Transition Contributions, and Weighting Factors of the Five Lowest-Energy Excited Singlet States of 2 and 3 at the B3LYP//Lanl2dz/6-31G*

excited state	λ_{abs}/nm (eV)	f[a]	transition contribution	weighing factor
		$[Ru(phen)_2(Hcdpq)]^{2+}$**2**		
^{1}ES1	462.1 (2.68)	0.0001	HOMO → LUMO	0.48932 (47.89%)[b]
			HOMO → LUMO+1	−0.44917 (40.35%)
			HOMO → LUMO+3	−0.21474 (9.22%)
^{1}ES2	438.3 (2.83)	0.0011	HOMO−1 → LUMO	0.50940 (51.90%)
			HOMO−1 → LUMO+1	−0.41340 (34.18%)
			HOMO−1 → LUMO+3	−0.18621 (6.93%)
^{1}ES3	434.5 (2.85)	0.0048	HOMO → LUMO+4	0.37064 (27.47%)
			HOMO → LUMO+1	−0.35752 (25.56%)
			HOMO → LUMO	−0.35239 (24.84%)
			HOMO−2 → LUMO	−0.17839 (6.36%)
			HOMO → LUMO+2	−0.16663 (5.55%)
^{1}ES4	431.9 (2.87)	0.0009	HOMO → LUMO+2	0.49854 (49.71%)
			HOMO → LUMO+3	0.32375 (20.96%)
			HOMO → LUMO+1	−0.31578 (19.94%)
			HOMO → LUMO+4	−0.17253 (5.95%)
^{1}ES5	431.1 (2.88)	0.0075	HOMO → LUMO+4	0.43817 (38.40%)
			HOMO → LUMO	0.32100 (20.61%)
			HOMO → LUMO+3	0.30984 (19.20%)
			HOMO → LUMO+1	0.20178 (8.14%)
			HOMO−2 → LUMO	−0.16722 (5.59%)
		$[Ru(phen)_2(cdpq)]^{+}$**3**		
^{1}ES1	446.8 (2.78)	0.0002	HOMO−1 → LUMO	0.57679 (66.54%)
			HOMO−1 → LUMO+1	−0.36720 (26.97%)
^{1}ES2	438.9 (2.82)	0.0001	HOMO−1 → LUMO+2	0.68640 (94.23%)
^{1}ES3	438.2 (2.83)	0.0007	HOMO−1 → LUMO+1	0.57227 (65.50%)
			HOMO−1 → LUMO	0.38582 (29.77%)
^{1}ES4	422.2 (2.94)	0.0028	HOMO−3 → LUMO	0.53773 (57.83%)
			HOMO−3 → LUMO+1	−0.35762 (25.58%)
^{1}ES5	417.5 (2.97)	0.1281	HOMO−2 → LUMO	0.41356 (34.21%)
			HOMO → LUMO	0.40762 (33.23%)
			HOMO−4 → LUMO	0.28437 (16.17%)

[a] Oscillator strength. [b] The percentage contributions to wave functions of excited states are given in parentheses.

deprotonation of carboxyl acid on Hcdpq promotes the energies of $-COO^-$ moiety and makes some frontier occupied MOs of **3**, such as HOMO, HOMO−2, and HOMO−4, to possess d_{Ru} character together with p orbitals of C and O atoms of $-COO^-$ moiety. Moreover, the LUMO of **3** is localized on the proximal bpy portion and N atoms of pyrazine rather than the whole cdpq as observed for **2** (Figure 1).

The electronic absorption spectra of **2** and **3** in neutral water in the vertical singlet excited states were also investigated by the TDDFT at the B3LYP//LanL2DZ/6-31G level. The calculated electronic absorption spectrum of **3** with oscillator strength (f) > 0.03 is shown in the Supporting Information, Figure S1. The energies, oscillator strengths, transition contributions, and weighting factors of five calculated lowest-lying excited singlet states of **2** and **3** are listed in Table 2. The transition contributions show that all of the five excited states in this table are ^{1}MLCT in character. The lowest-energy ^{1}MLCT states of **2** and **3** were calculated to be at 2.68 (462.1 nm, f = 0.0001) and 2.78 eV (446.8 nm, f = 0.0002), respectively. The strong transitions with f > 0.06 in the ^{1}MLCT band were listed in Table 3, together with transition contributions larger than 10%. The assignments in Table 3 show that all the transitions have ^{1}MLCT character originating from d_{Ru} orbits to both π^*_{phen} and π^*_{cdpq}. In addition, the broad-band absorption in the visible range also possesses some ^{1}IL (intraligand) and MC (metal-center) character, such as HOMO−2 → LUMO (34%, $d_{Ru} + \pi_{cdpq} \rightarrow \pi^*_{cdpq}$) at 417.5 nm and HOMO−3 → LUMO+1 (44%, $d_{Ru} \rightarrow \pi^*_{cdpq} + d_{Ru} + \pi^*_{phen}$) at 403.9 nm. It should be pointed out that the calculated wavelengths have an error of about 30 nm in comparison with the experimental data, which may be attributed to the limited precision of the TDDFT method as well as the approximate CPCM model for the solvent effect.

It has been proposed that the ^{3}MLCT transition from the Ru(II) to the distal phz part of the dppz ligand results in a nonemissive state, whereas the emissive state arises from a charge transfer from the Ru(II) center to the proximal bpy of dppz ligand or the ancillary ligands.[25,28,31,33] But the key factor that determines the BS/DS property of an excited state is whether the excited state possesses the phz nitrogen atomic orbital's character or not, because the hydrogen bonding between the phz nitrogen

dx.doi.org/10.1021/ic102126m |Inorg. Chem. 2011, 50, 6425–6436

Table 3. Some Significant Transitions ($f > 0.06$) in the ^{1}MLCT Band for 3, Together with Corresponding Assignment and Transition Contributions (> 10%) and the Experimental Maximum Absorption Wavelength (nm)

wavelength (nm)			
expt	calc	f [a]	assignment
442	417.5	0.1281	HOMO−2 → LUMO (34%)[b], $d_{Ru} + \pi_{cdpq} \rightarrow \pi^*_{cdpq}$
			HOMO → LUMO (33%), $d_{Ru} + \pi_{cdpq} \rightarrow \pi^*_{cdpq}$
			HOMO−4 → LUMO (16%), $d_{Ru} + \pi_{cdpq} \rightarrow \pi^*_{cdpq}$
	410.7	0.0752	HOMO−3 → LUMO+2 (25%), $d_{Ru} \rightarrow \pi^*_{phen} + d_{Ru}$
			HOMO → LUMO+1 (21%), $d_{Ru} + \pi_{cdpq} \rightarrow \pi^*_{cdpq} + d_{Ru} + \pi^*_{phen}$
			HOMO−2 → LUMO+1 (19%), $d_{Ru} + \pi_{cdpq} \rightarrow \pi^*_{cdpq} + d_{Ru} + \pi^*_{phen}$
			HOMO−4 → LUMO+1 (13%), $d_{Ru} + \pi_{cdpq} \rightarrow \pi^*_{cdpq} + d_{Ru} + \pi^*_{phen}$
			HOMO → LUMO (10%), $d_{Ru} + \pi_{cdpq} \rightarrow \pi^*_{cdpq}$
	403.9	0.1193	HOMO−3 → LUMO+1 (44%), $d_{Ru} \rightarrow \pi^*_{cdpq} + d_{Ru} + \pi^*_{phen}$
			HOMO−2 → LUMO+2 (19%), $d_{Ru} + \pi_{cdpq} \rightarrow \pi^*_{phen} + d_{Ru}$
	388.0	0.0668	HOMO−1 → LUMO+4 (86%), $d_{Ru} \rightarrow \pi^*_{phen}$
	349.8	0.1289	HOMO−4 → LUMO+5 (28%), $d_{Ru} + \pi_{cdpq} \rightarrow \pi^*_{cdpq}$
			HOMO−4 → LUMO+3 (11%), $d_{Ru} + \pi_{cdpq} \rightarrow \pi^*_{phen}$

[a] Oscillator strength. [b] The percentage contributions to the wave functions of the excited states are given in parentheses.

atoms and the solvent water would result in the decay of the excited state via nonradiative vibrational relaxation back to the ground state, and shut off the luminescence. For **2**, the electron density of the LUMO+1 is localized on the proximal bpy portion of Hcdpq, and the other four LUMOs (LUMO, LUMO+2, LUMO+3, and LUMO+4) have phz nitrogen atomic orbitals as their components. Therefore, it is expected that transitions from the Ru(II) center to the LUMO+1 would result in an emissive MLCT excited state, whereas MLCT excited states involving the LUMO, LUMO+2, LUMO+3, and LUMO+4 should be nonemissive or weakly emissive. Similarly, LUMO and LUMO+1 of **3** correspond to nonemissive or weakly emissive MLCT excited states, while the LUMO+2 of **3** corresponds to an emissive MLCT excited state.

It was proposed that MLCT states that possess >75% of nonemissive transitions should be assigned to DSs, BSs contained only emissive transitions, and these states that do not meet these criteria should be labeled mixed-states (MS).[33] And it was also assumed that the energy gap between the ^{1}MLCTs and corresponding ^{3}MLCTs of a Ru(II) polypyridyl complex is a constant,[33] such that the relative order of the MLCT states does not vary from the singlet to the triplet manifolds.[33,53] On the basis of the transition contributions and the weighting factors of the singlet excited states of **2** and **3** shown in Table 2, we can conclude that (1) for **2**, the first three lowest-lying triplet excited sates (^{3}ES1, ^{3}ES2, ^{3}ES3) are MSs, while ^{3}ES4 and ^{3}ES5 are DSs; (2) for **3**, ^{3}ES2 is BS, whereas the other four are DSs.

pH Effects on UV−visible Absorption and Emission Spectra. UV−visible spectrophotometric pH titrations were carried out over pH range from 0.50 to 11.02, and the pH effects on the UV−visible absorption spectra of the complex are shown in Supporting Information, Figure S2. On the basis of the comparisons of the spectra with those of $[Ru(phen)_3]^{2+}$ and the analogous complexes,[18,53] the band centered at ∼261 nm and the shoulder at ∼285 nm are assigned to the intraligand (IL) $^1\pi-\pi^*$ transitions, and the lowest-energy broad band centered at ∼440 nm to metal-to-ligand ($d_{Ru} \rightarrow \pi^*_{cdpq}$ and $d_{Ru} \rightarrow \pi^*_{phen}$) charge-transfer transition (^{1}MLCT). Both of the IL and the MLCT absorptions are typical features of polypyridyl Ru(II) complexes.[53] Supporting Information, Figure S2 reveals that the changes of the UV−visible spectra are negligibly weak, suggesting that the deprotonation of the carboxyl group of Hcdpq in **2** almost left unaffected both the IL $^1\pi-\pi^*$ and the ^{1}MLCT transitions.

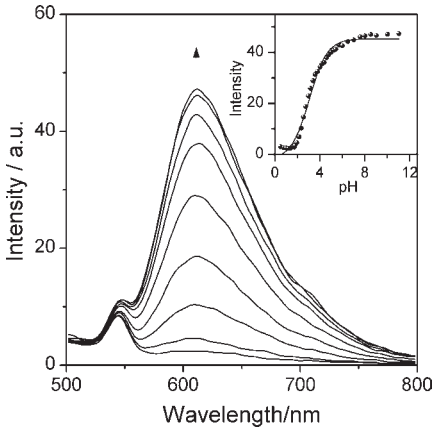

Figure 2. Changes in the emission spectra (λ_{ex} = 460 nm) of 4.42 μM $[Ru(phen)_2(Hcdpq)]^{2+}$ upon increasing pH 0.50 to 11.02. Arrows show spectral changes upon increasing the pH.

The emission spectral changes of **2** in aqueous solution as a function of pH are shown in Figure 2. In contrast to the UV−visible spectral behavior, the emission spectra are very sensitive to pH. In the acidic pH region 0.3−1.8, the complex almost had no luminescence. But further increases in pHs from 1.8 to 6.0 resulted in the excited-state deprotonation of carboxylic acid on **2** that switched "on" the solution luminescence by an intensity enhancement factor of 17. This large emission enhancement factor achieved over acidic pH region is comparable to a factor of 20 we previously reported for $[Ru(bpy)_2(Hbopip)]^{2+}$ {Hbopip = 2-(4-benzoxazolyl)phenylimidazo[4,5-*f*][1,10]phenanthroline},[40] 18−25 reported for $[Ru(bpy)_2(qtpy)]^{2+}$ (qtpy = 2,2′:3′,2″:6″,2‴-quaterpyridine), and $[Ru(bpy)_2(mqtpy)]^{2+}$ (mqtpy = 1‴-methyl-2,2′:3′,2″:6″,2‴-quaterpyridinium),[38] but less than a factor of 54 we reported for $[Ru(bpy)_2(btppz)]^{2+}$

dx.doi.org/10.1021/ic102126m |*Inorg. Chem.* 2011, 50, 6425–6436

Scheme 3. Ligand Fragment of cdpq (a); Rough Energy Level Diagrams of $[Ru(phen)_2(Hcdpq)]^{2+}$ in H_2O, and $[Ru(phen)_2(cdpq)]^{+}$ in H_2O and DNA (b)[a]

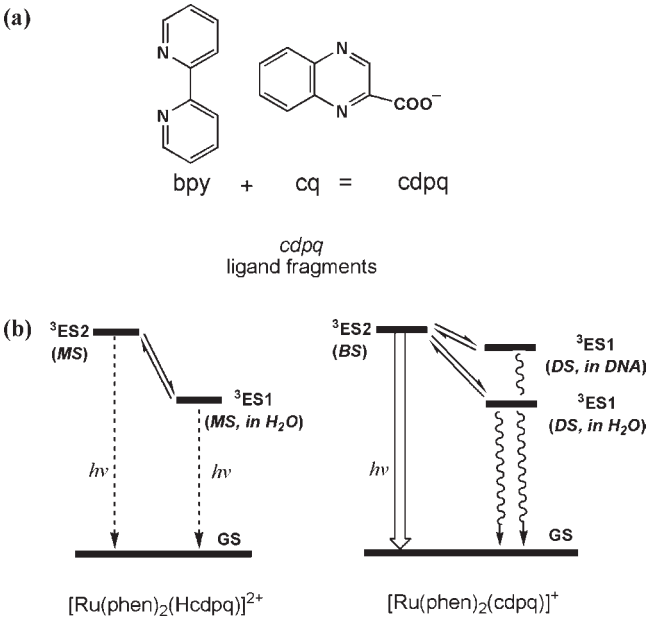

[a] ^{3}ES1: the lowest excited triplet state; ^{3}ES2: the second excited triplet state; GS: ground state; BS: bright state; DS: dark state; MS: mixed state.

{btppz = benzo[*h*]tripyrido[3,2-*a*:2′,3′-*c*:2″,3″-*j*]phenazine}.[43] The profile of emission intensities versus pH is shown in the inset of Figure 2. The monotone trend of the sigmoidal curve offers a clear proof of the existence of one excited-state protonation/deprotonation process of carboxylic acid of Hcdpq in **2** over the pH range studied. The negative logarithm value of an apparent acid ionization constant was derived to be pK_a = 3.06 ± 0.08 by a nonlinear sigmoidal fit of the data in the inset of Figure 2, which is reasonable as compared to pK_a values of 2.6 and 3.5 previously reported for $[Ru(phen)_2(Mebpy-COOH)]^{2+}$ (MebpyCOOH = 4′-methyl-2,2′-bipyridine-4-carboxylic acid)[63a] and $[Ru(bpy)_2(H_2dpqdc)]^{2+}$ {H_2dpqdc = dipyrido[3,2-*f*:2′,3′-*h*]quinoxaline-2,3-dicarboxylic acid},[63b] respectively.

It is well-known that the visible luminescence of Ru(II) polypyridyl complexes arises from the lowest ^{3}MLCT state. A rough sketch involving the two lowest ^{3}ESs of **2** in water, and those of **3** in both water and DNA is shown in Scheme 3. In the acidic pH region below 1.8, the complex exists as the protonated **2**, with its ^{3}ES1 and ^{3}ES2 being MS in character (Scheme 3b, left). Since these excited triplet states possess both emissive and nonemissive contributions, **2** would be weakly emissive,[33] consistent with experimental observation. Upon increasing pH, deprotonated **3** became the dominant species, and the ^{3}ES1 and ^{3}ES2 are changed to DS and BS, respectively (Scheme 3 b, right in H_2O). Despite that most of the excited states decay through the lowest triplet DS via a fast nonradiative relaxation back to the ground state, the transition equilibrium between BS and DS makes partial excited states deactivated from the ^{3}ES2, resulting in observable luminescence.

Calf Thymus DNA Binding Effects on UV−visible and Emission Spectra. According to the apparent pK_a value of 3.06 derived above, $[Ru(phen)_2(Hcdpq)]^{2+}$ exists as a deprotonated

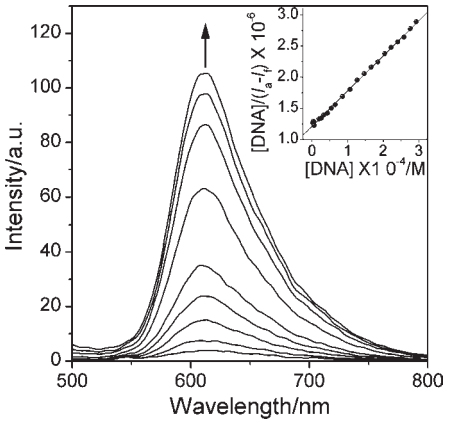

Figure 3. Changes in the emission spectra (λ_{ex} = 460 nm) of 2.69 μM $[Ru(phen)_2(cdpq)]^{+}$ with increasing concentrations of the DNA (0.00−292 μM) in buffered 50 mM NaCl (pH = 7.10). Inset: plots of $[DNA]/(I - I_0)$ vs [DNA] and the linear fit for the titration of the complex with the DNA.

form, $[Ru(phen)_2(cdpq)]^{+}$ **3**, under experimental condition for DNA bonding studies (pH 7 aqueous solution). The absorption spectra of **3** (2.69 μM) in the absence and the presence of increasing amounts of ct-DNA are illustrated in Supporting Information, Figure S3. During the DNA titration processes (from 0.00 to 254 μM), the absorption spectra of the complex were almost undisturbed, indicating that interaction of the complex with the DNA may be weak, and a classic intercalative binding may be excluded. The effects of successive additions of the DNA on the emission spectra of **3** are illustrated in Figure 3. In the absence of the DNA, the complex was weakly emissive (φ = 0.002). This is because in aqueous buffer, the formation of hydrogen bonds between the nitrogen atoms on pyrazine ring of cdpq and the H_2O molecules makes ^{3}ES1 (DS) significantly lower than ^{3}ES2 (BS, Scheme 3 b, right in H_2O), thus making the latter (BS) inefficiently thermally accessible. The energies of the excited state dissipate mainly from the DS via nonradiative vibrational relaxation back to the ground state, and weak luminescence was observed. Upon successive additions of the DNA, the luminescence of the complex revived sharply by 26- and 29.5-fold enhancements in emission intensity (I/I_0 = 26) and quantum yield (φ = 0.061) at [DNA]/[**3**] ≈ 220, respectively, behaving like some DNA molecular light switches.[7,20,43] Not only the DNA intercalators but also the groove-binders were reported to be capable of acting as DNA molecular light switches, for example, the ratios of emission intensity of the bound to the free form were reported to be 47 and 20−24 for intercalators of $[Ru(bpy)_2dppz]^{2+}$ and EB,[64a,b,65c] respectively, 140 for groove binder Hoescht 33258,[64a,b] less than 2 for Ru(II) complex-based groove binders of $[Ru(bpy)_2(mbpyeb)]^{2+}$ {mbpyeb = 4-[2-(4′-methyl-[2,2′-bipyridin]-4-yl)ethenyl]-1,2-benzenediol}, $[Ru(phen)_2(mbpyeb)]^{2+}$, and $[Ru(bpy)_2(phd)]^{2+}$ (Phd = 1,10-phenanthroline-5,6-diol).[64c] The emission enhancement of **3** in the presence of the DNA was also found to be associated with an increase in the lifetime of the excited Ru(II) complex from 14.9 ± 0.2 to 951.4 ± 6.9 ns as derived from fitting of the emission decay data to a single-exponential decay function (Supporting Information, Figure S4), namely, 63-fold excited state lifetime increase. These emission changes of $[Ru(phen)_2(cdpq)]^{+}$ induced by additions of the DNA clearly indicated that the Ru(II) was bound to the DNA. As addressed in the Introduction section, the protection of the

dx.doi.org/10.1021/ic102126m |*Inorg. Chem.* 2011, 50, 6425–6436

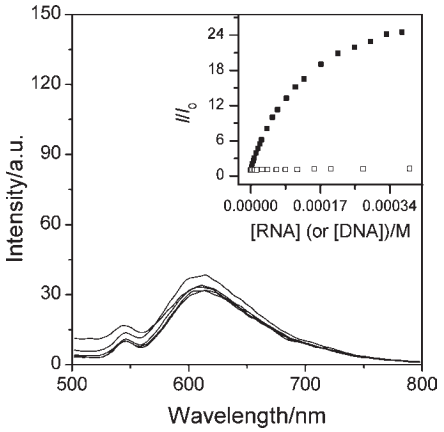

Figure 4. Changes in the emission spectra (λ_{ex} = 460 nm) of 2.69 μM $[Ru(phen)_2(cdpq)]^+$ with increasing concentrations of the RNA in buffered 50 mM NaCl (pH = 7.10). Inset: plots of I/I_0 vs [RNA] (hollow squares, from 0.00 to 389 μM) and [DNA] (solid squares, from 0.00 to 370 μM).

intercalative moieties by the DNA from forming intermolecular hydrogen bonds increased hydrophobility, the rigidity of the environment by DNA binding, and relative energy level position of BS and DS all may contribute to the DNA-induced emission enhancement observed.[5,7,23,31] As shown in Scheme 3, DNA binding may destabilize DS, making the energy gap between high-lying BS and low-lying DS for DNA-bound **3** significantly less than that for DNA-free **3**, and BS is thus easily accessible through thermal equilibrium, which enhances the radiative decay rate of BS, and accordingly the emission intensity.[24,28,31]

The intrinsic DNA binding constant, K_b, that illustrates the binding strength of the complex with ct-DNA, was obtained by monitoring the changes in luminescence intensity at 613 nm with increasing concentrations of the DNA, according to eq 2:

$$[DNA]/(I_a - I_f) = [DNA]/(I_b - I_f) + 1/K_b(I_b - I_f) \quad (2)$$

Where [DNA] is the concentration of DNA in base pairs, I_a is the luminescence intensities of the Ru(II) complex at given DNA concentrations, and I_b and I_f are the luminescence intensities for the ruthenium complex in the fully bound form and the free ruthenium complex, respectively. The ratio of the slope to the *y*-intercept in a plot of $[DNA]/(I_a - I_f)$ versus [DNA] shown in the inset of Figure 3 gave a K_b value of $(4.67 \pm 0.06) \times 10^3\ M^{-1}$, which is significantly less than a K_b value of $(1.4 \pm 0.2) \times 10^4\ M^{-1}$ for previously reported DNA intercalator $[Ru(phen)_2(dpq)]^{2+}$.[64a] This result is consistent with the optimized configuration of **3** by using the DFT-B3LYP method at the LanL2DZ/6-31G* level. It is well-known that the planarity of the main ligand plays a dominant role in determining the DNA-binding mode of a drug molecule. The COO^- moiety on $[Ru(phen)_2(cdpq)]^+$ has poor planarity with the dpq portion in cdpq ligand (N5−C6−C10−O11 = 126.19°, and N5−C6−C10−O12 = −53.91°) affording steric hindrance effect for the dpq portion to intercalate between the base pairs of the DNA. Furthermore, the electrostatic repulsion between the COO^- moiety and the negatively charged phosphate backbone of the DNA is also unfavorable for DNA binding.

The luminescence titration of **3** with yeast RNA (from 0.00 to 389 μM) was also performed, and the results are illustrated in Figure 4. Clearly, the addition of the RNA almost unaffected the emission spectrum of $[Ru(phen)_2(cdpq)]^+$, indicating an excellent DNA binding selectivity of **3** (also see inset of Figure 4). The RNA-binding experiments of two well-known DNA light switches of $[Ru(phen)_2(dppz)]^{2+}$ and EB were also performed for comparison (Supporting Information, Figures S5 and S6). The binding of $[Ru(phen)_2(dppz)]^{2+}$ and EB to the RNA resulted in evident changes both in UV−visible absorption and emission spectra. The binding of $[Ru(phen)_2(dppz)]^{2+}$ to the RNA was found to induce emission intensity enhancement factors of 3.3 and 16.8 at a low concentration of [Ru] = 0.41 μM, and a high concentration of [Ru] = 6.5 μM, respectively (Supporting Information, Figure S5). The binding of EB to the RNA elicited a large emission enhancement by a factor of 19 (Supporting Information, Figure S6). Obviously, the DNA binding selectivity of $[Ru(phen)_2(cdpq)]^+$ is superior to those of $[Ru(phen)_2(dppz)]^{2+}$ and EB.

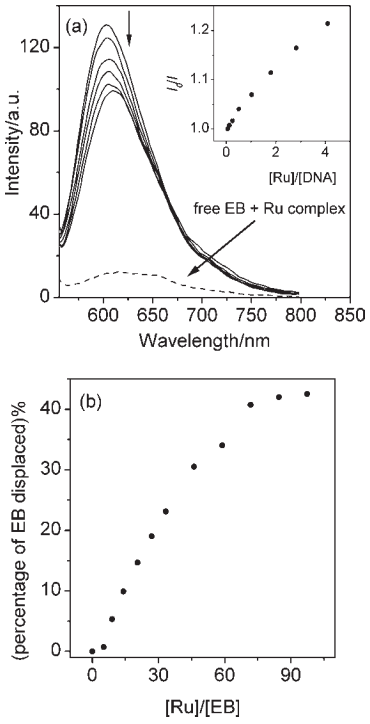

Figure 5. (a) Changes in emission spectra of EB (λ_{ex} = 537 nm) bound to DNA in the presence of $[Ru(phen)_2(cdpq)]^+$ (0.0−50.7 μM). The arrows show the intensity changes upon increasing concentrations of the complex. Inset: Stern−Volmer plot of quenching in the emission of DNA-bound EB by the complex; (b) Plot of percentage of EB displaced vs [Ru]/[EB]. [EB] = 0.6 μM, [DNA] = 3.0 μM, λ_{ex} = 537 nm.

Competitive Binding to the DNA with Ethidium Bromide. The competitive binding experiments with a well-established quenching assay[65a,b] based on the displacement of the intercalator ethidium bromide (EB) from ct-DNA-EB complex were carried out to get further information regarding the DNA binding properties of $[Ru(phen)_2(cdpq)]^+$. The free EB in aqueous solution is very weakly emissive (λ_{em} = 630 nm), but EB in the presence of the DNA displays a dramatic enhancement in emission intensity by a factor of 20 and a hypsochromic shift in the emission maximum to 605 nm (~540 nm excitation).[65c] It is generally accepted that the strong emission of the EB-DNA complex could be sharply reduced if a DNA intercalator is

dx.doi.org/10.1021/ic102126m |*Inorg. Chem.* 2011, 50, 6425–6436

successively added to the DNA pretreated with EB because of displacement of EB molecules inserted between the base pairs of DNA.[65d,e] It is noteworthy that as excited at λ_{ex} = 537 nm, not only free EB but also the Ru(II) complex in the free and bound forms are negligibly weakly emissive, facilitating the monitoring of the extent of the EB that is displaced from DNA bound EB. EB is generally regarded to be a strong DNA intercalator, but it was reported that it exhibits two types of binding modes to a genomic DNA depending upon the concentration ratio of [DNA]:[EB] and the solution ionic strength;[65f] weaker DNA binding at lower [DNA]:[EB] ratio ($K_b = 4 \times 10^4$ M^{-1}) and strong binding at higher [DNA]:[EB] ratio ($K_b = 100 \times 10^4$ M^{-1}).[65c] These two binding modes have also been verified by photoacoustic spectroscopy.[65g] These observations indicated that EB has two DNA binding modes, primarily intercalatively and partially groove bound to the DNA. EB was also reported to intercalate into DNA through interactions with the minor groove of the DNA; the displacement of EB by the titration of a drug is thus suggestive of an intercalative or minor groove binding.[65a,h−j] For example, the nonintercalating DNA groove binding agents of berenil, bisamidines, spermine, and spermidine were reported to be capable of displacing EB from DNA.[65k]But the reduction of DNA-bound EB emission is usually modest for the addition of a groove binder.[65k] Changes in the emission spectra of the DNA-bound EB upon increasing the concentration of **3** (Figure 5) showed that the reduction in emission of DNA-bound EB was very slow to a stable intensity at which only 40% of the DNA-bound EB molecules were displaced at very high concentration ratio [Ru]/[EB] = 90, in contrast to the evident reduction in the DNA-bound EB emission we previously reported by the additions of proven DNA intercalators of dpq moiety-containing $[Ru(bpy)_2(bipp)]^{2+}$, $[Ru(bpy)_2(bopp)]^{2+}$, and $[Ru(bpy)_2(btpp)]^{2+}$ {where bipp =2-benzimidazoyl-pyrazino[2,3-*f*][1,10]-phenanthroline, bopp = 2-benzoxazolyl-pyrazino[2,3-*f*][1,10]-phenanthroline, and btpp =2-benzthiazolyl-pyrazino[2,3-*f*]-[1,10]phenanthroline)}.[20] A quenching plot of I_0/I versus [Ru]/[DNA] (the inset of Figure 5a) is in good agreement with the linear Stern−Volmer equation $\{I_0/I = 1 + K_{SV}[Ru]\}$ with a Stern−Volmer quenching constant of $K_{SV} = (5.20 \pm 0.17) \times 10^{-2}$ M^{-1} that is much less than K_{SV} values of 5.24−40 M^{-1}we previously observed for DNA intercalators of $[Ru(bpy)_2(bipp)]^{2+}$, $[Ru(bpy)_2(bopp)]^{2+}$, $[Ru(bpy)_2(btpp)]^{2+}$, and $[Ru(bpy)_2(Hbopip)]^{2+}$ {Hbopip = 2-(4-benzoxazolyl)phenylimidazo[4,5-*f*][1,10]phenanthroline}.[20,40] To exclude the potential energy or/and energy transfer reactions between the DNA-bound EB and **3** that would cause the reduction in DNA bound EB emission, excited state lifetime measurements for the DNA bound EB in the absence and the presence of **3** were carried out with the same excitation and emission (610 nm) wavelengths as the EB competitive experiment, and the results are shown in the Supporting Information, Figure S7. The lifetimes of free EB and DNA-bound EB in the absence of **3** were found to be 2.11 ± 0.02 and 23.39 ± 0.08 ns, respectively, which are consistent to previously reported corresponding lifetimes of 1.67 and 23 ns.[65l] It is noteworthy that the presence of **3** almost unaffected the lifetime of DNA bound EB (22.96 ± 0.27 ns), indicating that the energy or/and energy transfer reactions between the DNA-bound EB and **3** can be excluded. This conclusion on the exclusion of the energy or/and electron transfer reactions is similar to that previously made on the addition of a Pt(II) complex of 2-hydroxy-ethanethiolato-(2,2′,2″-terpyridine)platinum(II) (PtTs) into DNA-bound EB

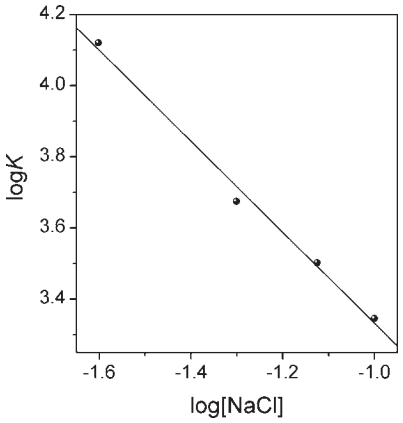

Figure 6. Plot of log $[Na^+]$ vs log K_{obs} in 5 mM Tris-HCl buffer solution. The slope of this plot corresponds to the $-Z\psi$ in eq 3.

{22.3 ± 0.5 ns in the absence of PtTs vs 21.85 ± 0.5 ns in the presence of PtTs}.[65m] Thus the slow emission reduction and partial displacement of EB from the DNA-EB complex observed by additions of **3** is ascribed to competition of **3** with EB for binding to the grooves of the DNA by formation of a nonemissive ternary complex of **3**-DNA-EB through simultaneous binding of groove binder **3** and intercalator EB to the DNA. The simultaneous binding of a minor groove binder Hoechst 33258 and intercalator EB to dodecamer DNA was previously verified.[65n]

Effects of Salt Concentrations on DNA Binding Constants. As anticipated from polyelectrolyte theory,[66] the interaction of positively charged Ru(II) complex with nucleic acids would be influenced by the presence of cations or the ionic strength of the solution.[67] The sensitivity to ionic strength was reported to decrease in the order of the DNA binding modes: electrostatic > groove > intercalative, which has proved in a qualitative and a quantitative manner to give information on the DNA binding mode. Since the polyelectrolyte theory is strictly applicable to the system with salt concentrations lower than 0.100 M, the NaCl concentrations were varied from 0.025 to 0.100 M in the DNA luminescence titration experiments. The DNA binding constant values derived at 25, 50, 75, and 100 mM NaCl, were (1.32 ± 0.12) × 10^4, (4.67 ± 0.05) × 10^3, (3.17 ± 0.05) × 10^3, and (2.21 ± 0.08) × 10^3 M^{-1}, respectively. The plot of log $[Na^+]$ against log K_{obs} (Figure 6) clearly shows that the DNA binding constant values decrease with increasing NaCl concentrations. This is due to the stoichiometry release of sodium ion following the binding of the Ru(II) complex to the DNA, suggesting that electrostatic interaction is involved in the DNA-binding event. The slope of linear fitting of Figure 5 is equal to $-Z\psi$ in the following equation:

$$-Z\psi = \delta \log K_{obs}/\delta \log [Na^+] \quad (3)$$

where Z is the charge on the Ru(II) complex, and ψ is the fraction of counterions associated with each DNA phosphate (ψ = 0.88 for double-stranded B-form DNA). A $Z\psi$ value of 1.27 ± 0.08 and a charge of 1.5 were thus derived. For structurally analogous DNA binders, the larger electrostatic contribution to the binding free energy change would usually result in a greater experimentally derived Z value. The Gibbs free energy change observed for DNA binding, ΔG_{obs}, can be

dx.doi.org/10.1021/ic102126m |*Inorg. Chem.* 2011, 50, 6425–6436

Table 4. Thermodynamic DNA Binding Parameters[a]

DNA binder[b]	binding mode	$K_{obs}/10^3$, M^{-1}	ΔG_{obs}, kJ mol^{-1}	Z	ΔG_{pe}, kJ mol^{-1}	ΔG_t ($\Delta G_t/\Delta G_{obs}$)	ref
ethidium bromide	intercalation	494	−32.2	0.85	−5.0	−27.2(0.85)	66
daynomycin	intercalation	4900	−37.7	0.95	−5.9	−31.8(0.84)	66
$[Ru(phen)_2(dppz)]^{2+}$	intercalation	3200	−37.2	2.15	−13.8	−23.4(0.63)	68
$[Ru(phen)_3]^{2+}$	groove binding	9.7	−22.6	1.6	−10.0	−13.0(0.57)	69
$[Ru_2(bpy)_4(Mebpy)(CH_2)_7(Mebpy)]^{4+}$	electrostatic binding	780	−23.6	2.50	−16.0	−7.5(0.32)	66
$[Ru_2(bpy)_4(tpphz)]^{4+}$	electrostatic binding	51000	−43.5	4.03	−26.4	−17.2(0.39)	24
$[Ru(phen)_2(cdpq)]^{+}$	groove binding	4.67	−21.0	1.5	−9.5	−11.5(0.55)	this work

[a] In 50 mM NaCl, 5 mM Tris-HCl buffer at room temperature. [b] dppz = dipyrido[3,2-*a*:2′,3′-*c*]phenazine; phen = 1,10-phenanthroline; Mebpy = 4-methyl-2,2′-bipyridine; tpphz = tetrapyrido-[3,2-*a*:2′,3′-*c*:3″,2″-*h*:2‴,3‴-*j*]phenazine.

calculated on basis of the standard Gibbs eq 4:

$$\Delta G_{obs} = -RT\ ln\ K_{obs} \quad (4)$$

$$\Delta G_{pe} = Z\psi RT\ ln\ [Na^+] \quad (5)$$

$$\Delta G_t = \Delta G_{obs} - \Delta G_{pe} \quad (6)$$

ΔG_{obs} can be divided into two portions, electrostatic (ΔG_{pe}) and nonelectrostatic (ΔG_t) components, which can be calculated from eqs 5 and 6, respectively. The thermodynamic binding parameters of **3** along with those reported for related complexes are summarized in Table 4. It is evident from Table 4 that the contribution of nonelectrostatic component (55%) to the binding free energy change ΔG_{obs} is only moderately greater than the electrostatic component (45%). Clearly, the nonelectrostatic contributions to ΔG_{obs} for $[Ru(phen)_2(cdpq)]^+$ is much less than the dominant nonelectrostatic contributions (66−85%) previously reported for the classical DNA intercalators of EB, daynomycin, $[Ru(bpy)_2(bipp)]^{2+}$, $[Ru(bpy)_2(bopp)]^{2+}$, and $[Ru(bpy)_2(btpp)]^{2+}$ (where bpy = 2,2′-bipyridine, bipp = 2-benzimidazoyl-pyrazino[2,3-*f*][1,10]phenanthroline, bopp = 2-benzoxazolyl-pyrazino[2,3-*f*][1,10]phenanthroline, and btpp = 2-benzthiazolyl-pyrazino[2,3-*f*][1,10]phenanthroline),[20] but much higher than minor nonelectrostatic contributions (32−39%) previously reported for electrostatic binders of $[(bpy)_2Ru(tpphz)Ru(bpy)_2]^{4+}$ and $[(bpy)_2Ru(Mebpy)(CH_2)_7(Mebpy)Ru(bpy)_2]^{4+}$ (see Table 4).[24,66,68,69] The results for the complex are qualitatively similar to those of $[Ru(phen)_3]^{2+}$, a hydrophobic binder in the major groove,[69] which was reported to have a slightly greater contribution to ΔG_{obs} from nonelectrostatic binding free energy change ΔG_t (57%) than from electrostatic binding free energy change ΔG_{pe} (43%). The above results give a signature that $[Ru(phen)_2(cdpq)]^+$ is probably a groove DNA binder.

Viscosity Measurements. The optical studies cannot provide sufficient evidence to support the binding mode, while hydrodynamic measurements, such as viscosity and sedimentation, are critical tests for a binding mode in solution in the absence of crystallographic structural data. Therefore, the effects of the successive additions of **3** on the viscosities of aqueous ct-DNA solutions were investigated. Because DNA viscosities are sensitive to the length changes of nucleic acids, a classical intercalation mode should result in lengthening the DNA helix as base pairs are separated to accommodate the binding ligand, thus increasing in relative specific viscosity of DNA.[70] The electrostatic or groove binders[64c,71] {e.g., netropsin, distamycin, and $[Ru(bpy)_2(mbpyeb)]^{2+}$, $[Ru(phen)_2(mbpyeb)]^{2+}$, $[Ru(bpy)_2(phd)]^{2+}$}

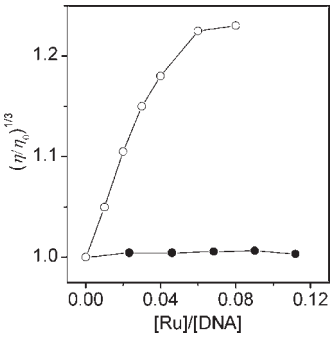

Figure 7. Changes in relative viscosities of ct-DNA (0.35 mM) upon successively increasing concentrations of $[Ru(phen)_2(cdpq)]^+$ (solid circles) and EB (hollow circles) at 31.66 ± 0.01 °C.

causes slight or no changes in DNA solution viscosity.[71] In contrast, a partial and/or nonclassical intercalation of ligand could bend (or kink) the DNA helix, reducing its effective length and concomitantly its viscosity.[70,72] The changes of the relative viscosities of ct-DNA upon increasing amounts of **3** and the well-known DNA intercalator EB are shown in Figure 7. Clearly, in contrast to the case of intercalator EB, the additions of increasing concentrations of **3** to 0.35 mM ct-DNA did not result in an increase in the relative viscosities of the DNA; thus an intercalative DNA binding mode could unequivocally be excluded.

CONCLUSIONS

A novel Ru(II) complex of $[Ru(phen)_2(Hcdpq)](ClO_4)_2$ has been synthesized and characterized. The pH and ct-DNA luminescence titrations of $[Ru(phen)_2(cdpq)]^+$ showed that the complex acted as a dual molecular light switch for pH (I/I_0 = 17) with an apparent acid ionization constant of $pK_a = 3.06 \pm 0.08$, and for DNA (I/I_0 = 26) with a small DNA binding constant on the order of magnitude of 10^3 M^{-1} in buffered 50 mM NaCl aqueous solution (pH 7.1). Another interesting feature that is noteworthy to mention is that $[Ru(phen)_2(cdpq)]^+$ is capable of distinguishing ct-DNA from yeast RNA with this selectivity being superior to two well-known DNA light switches of $[Ru(bpy)_2(dppz)]^{2+}$ and ethidium bromide. Almost unchanged DNA viscosities by additions of $[Ru(phen)_2(cdpq)]^+$ suggested that an intercalative DNA binding mode can be excluded. $[Ru(phen)_2(cdpq)]^+$ was found to partially displace EB from DNA-EB complex, which is distinct from almost full displacement of the EB by analogous DNA intercalators of $[Ru(bpy)_2(bipp)]^{2+}$, $[Ru(bpy)_2(bopp)]^{2+}$, and $[Ru(bpy)_2(btpp)]^{2+}$,[20] indicative of a groove binding of $[Ru(phen)_2(cdpq)]^+$ to the DNA. Also,

dx.doi.org/10.1021/ic102126m |*Inorg. Chem.* 2011, 50, 6425–6436

$[Ru(phen)_2(cdpq)]^+$ was found to have a moderately greater nonelectrostatic contribution (55%) to DNA binding free energy change than the electrostatic contribution (45%), distinctly different from dominantly nonelectrostatic contributions previously reported for classical DNA intercalators. These facts led us to make a conclusion that groove binding is a main mode for $[Ru(phen)_2(cdpq)]^+$. This study has also provided an example that "intercalation is not absolutely required for DNA light-switch behavior".[33] The geometry optimizations and computations of electronic structures by applying the DFT-B3LYP method at the LanL2DZ/6-31G* level revealed that (1) the COOH group on $[Ru(phen)_2(Hcdpq)]^{2+}$ remains coplanar with dpq ring; (2) the deprotonation of the COOH group of $[Ru(phen)_2(Hcdpq)]^{2+}$ renders poor planarity of dpq and carboxylate anion in $[Ru(phen)_2(cdpq)]^+$, which is unfavorable for $[Ru(phen)_2(cdpq)]^+$ to intercalate into the DNA. The deprotonation also leads to an evident destabilization of dpq and COO^- moiety-localized orbitals. The DFT/TDDFT calculated ground- and vertical singlet excited-states for **2** and **3** provide a reasonable explanation for the dual light-switch mechanism.

■ ASSOCIATED CONTENT

Supporting Information. The calculated electronic absorption Spectrum of **3** over 250−500 nm and oscillator strengths (*f*) using the TDDFT method in water with CPCM model, the effects of increases in pH from 0.5 to 11.20 on the UV−visible spectra of $[Ru(phen)_2(Hcdpq)]^{2+}$ (4.42 μM) in Britton-Robinson, changes in absorption spectra of $[Ru(phen)_2(cdpq)]^+$ (2.69 μM) upon addition of ct-DNA (0.00−254.05 μM) in buffered 50 mM NaCl (pH = 7.10), changes in the absorption and emission spectra of varied concentrations of $[Ru(phen)_2(dppz)]^{2+}$ with increasing concentrations of the RNA in 5 mM Tris-HCl, changes in the absorption spectra and emission spectra (λ_{ex} = 537 nm) of EB (10 μM) with increasing concentrations of RNA (0−650 μM) in 5 mM Tris-HCl (50 mM NaCl, pH = 7.10), and single-exponential fit of the emission decay data at λ_{em} = 610 nm (λ_{ex} = 537 nm) of EB-DNA system ([EB] = 20 μM, [DNA] = 100 μM) in the absence (a) and the presence (b) of 40 μM $[Ru(phen)_2(cdpq)]^+$. This material is available free of charge via the Internet at http://pubs.acs.org.

■ AUTHOR INFORMATION

Corresponding Author

*E-mail: kzwang@bnu.edu.cn. Fax: +86-10-62200567. Phone: +86-10-62205476.

■ ACKNOWLEDGMENT

The authors thank the National Natural Science Foundation (20771016, 20971016, and 90922004), Beijing Natural Science Foundation (2072011), The Fundamental Research Funds for the Central Universities, and Analytical and Measurements Fund of Beijing Normal University for financial supports.

■ REFERENCES

(1) Balzani, V.; Credi, A.; Venturi, M. *ChemSusChem* **2008**, *1*, 26.
(2) Dalton, S. R.; Glazier, S.; Leung, B.; Win, S.; Megatulski, C.; Burgmayer, S. J. N. *J. Biol. Inorg. Chem.* **2008**, *13*, 1133.
(3) Spillane, C. B.; Fletcher, N. C.; Rountree, S. M.; van den Berg, H.; Chanduloy, S.; Morgan, J. L.; Keene, F. R. *J. Biol. Inorg. Chem.* **2007**, *12*, 797.
(4) Zou, X. H.; Ye, B. H.; Li, H.; Zhang, Q. L.; Chao, H.; Liu, J. G.; Ji, L. N.; Li, X. Y. *J. Biol. Inorg. Chem.* **2001**, *6*, 143.
(5) Barton, J. K. *Science* **1986**, *233*, 727.
(6) Metcalfe, C.; Thomas, J. A. *Chem. Soc. Rev.* **2003**, *32*, 215.
(7) Friedman, A. E.; Chambron, J. C.; Sauvage, J. P.; Turro, N. J.; Barton, J. K. *J. Am. Chem. Soc.* **1990**, *112*, 4960.
(8) Hartshorn, R. M.; Barton, J. K. *J. Am. Chem. Soc.* **1992**, *114*, 5919.
(9) Erkkila, K. E.; Odom, D. T.; Barton, J. K. *Chem. Rev.* **1999**, *99*, 2777.
(10) Ruba, E.; Hart, J. R.; Barton, J. K. *Inorg. Chem.* **2004**, *43*, 4570.
(11) Dupureur, C. M.; Barton, J. K. *J. Am. Chem. Soc.* **1994**, *116*, 10286.
(12) Delaney, S.; Pascaly, M.; Bhattarcharya, P.; Han, K.; Barton, J. K. *Inorg. Chem.* **2002**, *41*, 1966.
(13) Dupureur, C. M.; Barton, J. K. *Inorg. Chem.* **1997**, *36*, 33.
(14) Jenkins, Y.; Friedman, A. E.; Turro, N. J.; Barton, J. K. *Biochemistry* **1992**, *31*, 10809.
(15) Rajput, C.; Rutkaite, R.; Swanson, L.; Haq, I.; Thomas, J. A. *Chem.—Eur. J.* **2006**, *12*, 4611.
(16) O'Donoghue, K. A.; Penedo, J. C.; Kelly, J. M.; Kruger, P. E. *Dalton Trans* **2005**, 1123.
(17) Collins, J. G.; Sleeman, A. D.; Aldrich-Wright, J. R.; Greguric, I.; Hambley, T. W. *Inorg. Chem.* **1998**, *37*, 3133.
(18) Ambroise, A.; Maiya, B. G. *Inorg. Chem.* **2000**, *39*, 4264.
(19) O'Donoghue, K. A.; Kelly, J. M.; Kruger, P. E. *Dalton Trans* **2004**, 13.
(20) Han, M. J.; Duan, Z. M.; Hao, Q.; Zheng, S. Z.; Wang, K. Z. *J. Phys. Chem. C* **2007**, *111*, 16577.
(21) Zhen, Q. X.; Ye, B. H.; Zhang, Q. L.; Liu, J. G.; Li, H.; Ji, L. N. *J. Inorg. Biochem.* **1999**, *76*, 47.
(22) Li, J.; Chen, J. C.; Xu, L. C.; Zheng, K. C.; Ji, L. N. *J. Organomet. Chem.* **2007**, *692*, 831.
(23) Mariappan, M.; Maiya, B. G. *Eur. J. Inorg. Chem.* **2005**, 2164.
(24) Lutterman, D. A.; Chouai, A.; Liu, Y.; Sun, Y.; Stewart, C. D.; Dunbar, K. R.; Turro, C. *J. Am. Chem. Soc.* **2008**, *130*, 1163.
(25) Olson, E. J. C.; Hu, D.; Hormann, A.; Jonkman, A. M.; Arkin, M. R.; Stemp, E. D. A.; Barton, J. K.; Barbara, P. F. *J. Am. Chem. Soc.* **1997**, *119*, 11458.
(26) Nair, R. B.; Cullum, B. M.; Murphy, C. J. *Inorg. Chem.* **1997**, *36*, 962.
(27) Coates, C. G.; Callaghan, P. L.; Mcgarvey, J. J.; Kelly, J. M.; Kruger, P. E.; Higgins, M. E. *J. Raman Spectrosc.* **2000**, *31*, 283.
(28) Brennaman, M. K.; Alstrum-Acevedo, J. H.; Fleming, C. N.; Jang, P.; Meyer, T. J.; Papanikolas, J. M. *J. Am. Chem. Soc.* **2002**, *124*, 15094.
(29) Olofsson, J.; Onfelt, B.; Lincoln, P. *J. Phys. Chem. A* **2004**, *108*, 4391.
(30) Batista, E. R.; Martin, R. L. *J. Phys. Chem. A* **2005**, *109*, 3128.
(31) Brennaman, M. K.; Meyer, T. J.; Papanikolas, J. M. *J. Phys. Chem. A* **2004**, *108*, 9938.
(32) Pourtois, G.; Beljonne, D.; Moucheron, C.; Schumm, S.; Mesmaeker, A. K. D.; Lazzaroni, R.; Brédas, J. L. *J. Am. Chem. Soc.* **2004**, *126*, 683.
(33) Sun, Y. J.; Lutlerman, D. A.; Turro, C. *Inorg. Chem.* **2008**, *47*, 6427.
(34) Stryer, L. *Biochemistry*, Freeman: New York, 1988.
(35) Yam, V. W. W.; Kai, A. S. F. *Inorg. Chim. Acta* **2000**, *82*, 300.
(36) Haga, M. A.; Takasugi, T.; Tomie, A.; Ishizuya, M.; Yamada, T.; Hossain, M. D.; Inoue, M. *Dalton Trans* **2003**, 2069.
(37) Allardyce, C. S.; Dyson, P. J.; Ellis, D. J.; Heath, S. L. *J. Chem. Soc., Chem. Commun.* **2001**, 1396.
(38) Guardigli, M.; Flamigni, L.; Barigelletti, F.; Richards, C. S. W.; Ward, M. D. *J. Phys. Chem.* **1996**, *100*, 10620.
(39) Liu, F. R.; Wang, K. Z.; Bai, G. Y.; Zhang, Y. A.; Gao, L. H. *Inorg. Chem.* **2004**, *43*, 1799.

(40) Han, M. J.; Gao, L. H.; Lü, Y. Y.; Wang, K. Z. *J. Phys. Chem. B* **2006**, *110*, 2364.
(41) Gao, F.; Chao, H.; Zhou, F.; Peng, B.; Ji, L. N. *Inorg. Chem. Commun.* **2007**, *10*, 170.
(42) Cheng, F. X.; Tang, N. *Inorg. Chem. Commun.* **2008**, *11*, 506.
(43) Chen, Y. M.; Liu, Y. J.; Li, Q.; Wang, K. Z. *J. Inorg. Biochem.* **2009**, *103*, 1359.
(44) Fan, S. H.; Wang, K. Z.; Yang, W. C. *Eur. J. Inorg. Chem.* **2009**, 508.
(45) Bashford, D.; Karplus, M. *Biochemistry* **1990**, *29*, 10219.
(46) Ma, Y. Z.; Yin, H. J.; Wang, K. Z. *J. Phys. Chem. B* **2009**, *113*, 11039.
(47) Delgadillo, A.; Romo, P.; Leiva, A. M.; Leob, B. *Helv. Chim. Acta* **2003**, *86*, 2110.
(48) Ji, Z. Q.; Huang, S. P.; Guadalupe, A. R. *Inorg. Chim. Acta* **2000**, *305*, 127.
(49) Perrin, D. D.; Armarego, W. L.; Perrin, D. R. *Purification of Laboratory Chemicals*, 2nd ed.; Pergamon: Oxford, 1980.
(50) Houten, J. V.; Watts, R. J. *J. Am. Chem. Soc.* **1976**, *98*, 4853.
(51) Chaires, J. B.; Dattagupta, N.; Crothers, D. M. *Biochemistry* **1982**, *21*, 3933.
(52) Zou, X. H.; Ye, B. H.; Li, H.; Liu, J. G.; Xiong, Y.; Ji, L. N. *J. Chem. Soc., Dalton Trans.* **1999**, 1424.
(53) Juris, A.; Balzani, V.; Barigelletti, F.; Campagna, S.; Belser, P.; von Zelewsky, A. *Coord. Chem. Rev.* **1988**, *84*, 85.
(54) Barone, V.; Cossi, M. *J. Phys. Chem. A* **1998**, *102*, 1995.
(55) Cossi, M.; Rega, N.; Scalmani, G.; Barone, V. *J. Comput. Chem.* **2003**, *24*, 669.
(56) Lee, C.; Yang, W.; Parr, R. G. *Phys. Rev. B: Condens. Matter Mater. Phys.* **1988**, *37*, 785.
(57) Becke, A. D. *Phys. Rev. A: Gen. Phys.* **1988**, *38*, 3098.
(58) Becke, A. D. *J. Chem. Phys.* **1993**, *98*, 5648.
(59) Hehre, W. J.; Radom, L.; Schleyer, P.V. R.; Pople, J. A. *Ab Initio Molecular Orbital Theory*; Wiley & Sons: New York, 1986.
(60) Hay, P. J.; Wadt, W. R. *J. Chem. Phys.* **1985**, *82*, 270.
(61) Wadt, W. R.; Hay, P. J. *J. Chem. Phys.* **1985**, *82*, 284.
(62) Frisch, M. J. *Gaussian 03*, Revision D.01; Gaussian Inc: Wallingford, CT, 2005.
(63) (a) Su, C. H.; Chen, H. Y.; Tsai, K. Y. D.; Chang, I. J. *J. Phys. Chem. B* **2007**, *111*, 6857. (b) Gholamkhass, B.; Koike, K.; Negishi, N.; Hori, H.; Takeuchi, K. *Inorg. Chem.* **2001**, *40*, 756.
(64) (a) Urathammakul, T.; Waller, D. J.; Beck, J. L.; Aldrich-Wright, J. R.; Ralph, S. F. *Inorg. Chem.* **2008**, *47*, 6621. (b) Suh, D.; Chaires, J. B. *Bioorg. Med. Chem.* **1995**, *3*, 723. (c) Ghosh, A.; Das, P.; Gill, M. R.; Kar, P.; Walker, M. G.; Thomas, J. A.; Das, A. *Chem.—Eur. J.* **2011**, *17*, 2089.
(65) (a) Boger, D. L.; Fink, B. E.; Brunette, S. R.; Tse, W. C.; Hedric, M. P. *J. Am. Chem. Soc.* **2001**, *123*, 5878. (b) Boger, D. L.; Fink, B. E.; Hedrick, M. P. *J. Am. Chem. Soc.* **2000**, *122*, 6382. (c) Sarkar, R.; Pal, S. K. *Biopolymers* **2006**, *83*, 675. (d) Tsai, C. C.; Jain, S. C.; Sobell, H. M. *Proc. Natl. Acad. Sci. U.S.A.* **1975**, *72*, 628. (e) Breslauer, K. J.; Remeta, D. P.; Chou, W. Y.; Ferrante, R.; Curry, J.; Zaunczkowski, D.; Snyder, J. G.; Marky, L. A. *Proc. Natl. Acad. Sci. U.S.A.* **1987**, *84*, 8922. (f) Vardevanyan, P. O.; Antonyan, A. P.; Parsadanyan, M. A.; Davtyan, H. G.; Karapetyan, A. T. *Exp. Mol. Med.* **2003**, *35*, 527. (g) Bugs, M. R.; Cornélio, M. L. *Eur. Biophys. J.* **2002**, *31*, 232. (h) Baguley, B. C.; Falkenhaug, E. M. *Nucleic Acids Res.* **1978**, *5*, 161. (i) Palchaudhuri, R.; Hergenrother, P. J. *Curr. Opin. Biotechnol.* **2007**, *18*, 497. (j) Shim, Y. H.; Arimondo, P. B.; Laigle, A.; Garbesi, A.; Lavielle, S. *Org. Biomol. Chem.* **2004**, *2*, 915. (k) Cain, B. F.; Baguley, B. C.; Denny, W. A. *J. Med. Chem.* **1978**, *21*, 658. (l) Heller, D. P.; Greenstock, C. L. *Biophys. Chem.* **1994**, *50*, 305. (m) Jennette, K. W.; Lippard, S. J.; Vassiliades, G. A.; Baueri, W. R. *Proc. Natl. Acad. Sci. U.S.A.* **1974**, *71*, 3839. (n) Banerjee, D.; Pal, S. K. *J. Phys. Chem. B* **2007**, *111*, 5047.
(66) Mudasir, W. K.; Wahyuni, E. T.; Yoshioka, N.; Inoue, H. *Biophys. Chem.* **2006**, *121*, 44.
(67) Record, M. T.; Lohman, T. M.; De Haseth, P. *J. Mol. Biol.* **1976**, *107*, 145.
(68) Pierard, F.; Guerzo, A. D.; Kirsch-De Mesmaeker, A.; Demeunynck, M.; Lhomme, J. *Phys. Chem. Chem. Phys.* **2001**, *3*, 2911.
(69) Satyanarayana, S.; Dabrowiak, J. C.; Chaires, J. B. *Biochemistry* **1992**, *31*, 9319.
(70) Lü, Y. Y.; Gao, L. H.; Han, M. J.; Wang, K. Z. *Eur. J. Inorg. Chem.* **2006**, 430.
(71) Lerman, L. *J. Mol. Biol.* **1961**, *3*, 18.
(72) Satyanarayana, S.; Dabrowiak, J. C.; Chaires, J. B. *Biochemistry* **1993**, *32*, 2573.